Experimental and theoretical study of electron momentum density of A_nC_{60} ($n=3,4$) and comparison to pristine C_{60}

M. Marangolo, Ch. Bellin, and G. Loupias*
Laboratoire de Minéralogie-Cristallographie de Paris, Université de Paris VI et VII, URA CNRS 7590, case 115, 4 place Jussieu, 75252 Paris Cedex 05, France

S. Rabii
Department of Electrical Engineering, University of Pennsylvania, Philadelphia, Pennsylvania 19104-6390

S. C. Erwin
Complex Systems Theory Branch, NRL, Washington, DC 20375

Th. Buslaps
European Synchrotron Radiation Facility (ESRF), Boîte Postale 220, 38043 Grenoble-Cedex, France
(Received 1 April 1999)

Compton profile measurements on K_nC_{60} ($n=3$ and 4), $CsRb_2C_{60}$, Rb_4C_{60}, and C_{60} powders have been carried out using inelastically scattered photons. We compare the experimental Compton profile difference (CPD) of K_nC_{60} ($n=3,4$) and that of C_{60} with the corresponding calculated results, obtained from *ab initio* self-consistent field calculations of the energy band structure. This permits us to isolate the contribution of the distortion of the C_{60} orbitals for each compound and to compare them, as a function of alkali intercalation. For all the samples we have obtained an overall agreement between theory and experiment. Nevertheless, in the case of K_4C_{60}, the comparison between the calculated and measured CPD's widths is not satisfactory. The calculated width is larger than the experimental results. Furthermore, similar measurements performed on heavy ions intercalated compounds (Rb_4C_{60} and Rb_2CsC_{60}) show clearly that CPD depends on the number of ions and not on their nature. We put forward two possible hypotheses in order to explain the mismatch between theoretical and experimental CPD's of K_4C_{60}: (1) The orientations of C_{60} molecules in these compounds vary with n and they are not taken in account by calculations. (2) Jahn-Teller effect for the negatively charged C_{60} molecule in the solid. [S0163-1829(99)12447-0]

I. INTRODUCTION

The family of compounds, A_nC_{60} ($A=$K, Rb, and Cs; $n=1$, 3, 4, and 6) exhibit a diversity of structural and electronic properties which has made them subject of a great deal of interest. They exhibit conductivities ranging from superconducting to metallic to insulating as a function of alkali ion concentration. The orientations of C_{60} molecules in these compounds also vary with n. They are completely, ordered in K_6C_{60},[1] randomly occupy sites with two inequivalent orientations in K_3C_{60} (Ref. 2) and K_4C_{60},[3] and polymerize to form chains in K_1C_{60}.[4]

We have already reported on our investigation of momentum density in C_{60} (Ref. 5) and K_6C_{60} (Ref. 6) and in this work we extend our experimental and theoretical studies to K_3C_{60}, K_4C_{60}, Rb_2CsC_{60}, and Rb_4C_{60}. The wave functions obtained from *ab initio* energy band calculation of these compounds are used to calculate directional Compton profiles, which are the projections of electron momentum density along specific directions. Experimentally, inelastic scattering of x-rays from powder samples is used to measure an averaged Compton profile. Experimental and theoretical studies of electronic structure in momentum space are particularly suited for investigation of valence electrons in solids due to their extended nature. Furthermore, the incoherent nature of the x-rays inelastic scattering makes this approach ideally suited in cases where high-quality samples are not available.

Since the information provided by Compton scattering about the ground-state electron distribution can be directly related to the Fourier expansion of the wave function, this approach can be used as a direct probe of the quality of the calculated wave functions.

Sections II and III present Compton scattering and the theoretical approach. Section IV presents the experimental procedures, including sample preparation and characterization. Results and discussions are presented in Sec. V and conclusions given in Sec. VI.

II. COMPTON SCATTERING METHOD

When photons are inelastically scattered by electrons, the wavelength shift of the photons can be related to scattering angle and the initial momentum of electrons through conservation of energy and momentum. The resulting shift is given by

$$\Delta\lambda = \frac{2h}{mc}\sin^2\left(\frac{\varphi}{2}\right) + \frac{2\lambda_1}{mc}\sin\left(\frac{\varphi}{2}\right)q, \qquad (1)$$

where ϕ is the scattering angle, λ_1 the incoming beam wavelength, and q is the value of the initial electron momentum in the scattering direction.

The first term, i.e., the Compton shift, is simply the result of photons scattered by electrons at rest. The information about the ground state momentum density is contained in the second term, which is a broadening of the Compton peak due to the motion of the electrons.

In the impulse approximation (IA), one assumes that the scattering is fast enough so that the interaction potential can be regarded as unchanged during the process. Within this approximation, the Compton profile is defined as

$$J(q,\mathbf{e}) = \int n(\mathbf{p})\,\delta(\mathbf{p}\cdot\mathbf{e}-q)\,d\mathbf{p} = \int \chi^*(\mathbf{p})\chi(\mathbf{p})\,\delta(\mathbf{p}\cdot\mathbf{e}-q)\,d\mathbf{p}, \tag{2}$$

where $\mathbf{e}$ is the unit vector along the scattering vector $\mathbf{K}$, $n(\mathbf{p})$ is the electron momentum density and $\chi(\mathbf{p})$ is the wave function of the electron in momentum space, i.e., the Fourier transform of the wave function in real space.[7–9] Throughout the remainder of this paper we shall use atomic units (a.u.), for which $\hbar = m = 1$.

III. THEORETICAL APPROACH

The electronic structure of C_{60},[10] K_3C_{60},[11] and K_4C_{60} (Ref. 12) were calculated within the local density approximation using the Ceperly-Adler exchange-correlation functional. The Kohn-Sham equations were solved using the *ab initio* linear combination of atomic orbitals method. The localized orbitals were expanded on a set of Gaussian-orbital basis functions. The basis set for carbon included $4s$-type and $3p$-type Gaussian functions while for potassium it contained five *s*-type and four *p*-type functions. The calculations were self consistent, with no restrictions on the form of charge density or potential. Due to the large size of the unit cell, a single k point (Γ) was sufficient to achieve convergence in the Brillouin Zone (BZ) integration. The details of the formalism are given in Ref. 13.

The calculated ground-state wave functions are represented by their plane-wave expansion,

$$\psi_{n,\mathbf{k}}(\mathbf{r}) = \sum_{\mathbf{G}} C_{n,\mathbf{k}}(\mathbf{G}) \exp[i(\mathbf{k}+\mathbf{G})\cdot\mathbf{r}], \tag{3}$$

where $\mathbf{G}$'s are reciprocal lattice vectors. The large sizes of the primitive unit cells for these compounds result in very short lengths of the reciprocal lattice vectors. Therefore the number of G's necessary to obtain convergence in this sum is large. This number was 32 000 in this case as compared to 2000 in graphite.[5] Using this expansion in Eq. (2) results in the following form for the directional Compton profile

$$J(q,\mathbf{e}) = \frac{1}{N}\sum_{n}\sum_{\mathbf{k}}\sum_{\mathbf{G}} |C_{n,\mathbf{k}}(\mathbf{G})|^2\,\delta[(\mathbf{k}+\mathbf{G})\cdot\mathbf{e}-q]\,\vartheta \times (E_n - E_f). \tag{4}$$

The summation $\mathbf{G}$ is over all the reciprocal lattice vectors for which the $C_{n,k}(\mathbf{G})$'s are non-negligible. Summation $\mathbf{k}$ is over the symmetry-reduced sector of the Brillouin Zone (BZ) of each compound, using a tetrahedral interpolation method.[14] The volume of this irreducible sector of the BZ is divided into tetrahedra by choosing a grid of $\mathbf{k}$ points. The actual wave functions are calculated at each grid point and a linear interpolation is carried out for $|C_{n,k}(G)|^2$ within each tetrahedron. Due to the small volume of the BZ for these compounds, a relatively coarse mesh is sufficient for the BZ integration, 11 $\mathbf{k}$-points for K_3C_{60} and 13 for K_4C_{60}. The summation n is over the occupied states. The function θ cuts off this summation at the Fermi energy in the case where the material is a metal or a semimetal. Since the measurements are performed on powder samples, the comparison is made with the average theoretical profile obtained by calculating four directional profiles.

IV. EXPERIMENTAL PROCEDURE

A. Sample preparation and characterization

C_{60} powder from the Hoechst company is used in this study. Before its intercalation, the powder that contains some impurities, in particular sulfur, is meticulously purified. This purification consists of a very slow outgassing under high vacuum, from room temperature to 400 °C. The temperature is progressively increased, so that the pressure remains lower than 10^{-5} mm Hg. The process takes four to six weeks. XANES (x-ray absorption near edge structures) study was used to show that this treatment has removed all impurities, even oxygen, completely.[15] After outgassing, the powder is transferred under a pure argon atmosphere to avoid any oxygen contamination.

The saturated K_6C_{60} compound is prepared by reaction of an excess amount of alkali metal and by a weighed quantity of C_{60} powder (200 mg). The reaction is carried out in a vacuum-sealed Pyrex glass tube at 200 °C for 3 weeks. A gradient of a few degrees is maintained along the tube to prevent metal from condensing onto C_{60}. The x-ray powder diffraction pattern collected with Mo $K\alpha_1$ radiation shows clearly that all reflections can be indexed on a body centered cubic lattice with a parameter of $a = 11.39$ Å.

K_nC_{60} ($n = 3$ and 4) were produced by a solid state reaction between weighted quantities of C_{60} and K_6C_{60}. The reaction is carried out in a vacuum-sealed Pyrex glass tube for 2–3 months. The evolution of the reaction is controlled by x-ray diffraction until complete reaction of K_6C_{60} and hence disappearance.

B. Experimental set up

The experiments on K_nC_{60} ($n = 4$ and 6) and pristine C_{60} were carried out using the high-resolution spectrometer of the high-energy synchrotron at Laboratoire d'Utilisation du Rayonnement Electromagnétique in Orsay, France.[16] The positron storage ring operates at 1.85 GeV and a 3-pole superconducting magnet wiggler provides a beam with a critical energy of about 8 keV. The synchrotron radiation beam is monochromatized by Bragg reflection from a double Si(220) monochromator to produce a beam of energies up to 19 900 eV.[17] The beam is sagittally focused on the powder sample of K_4C_{60} by the monochromator's second crystal. The sample is a cylinder of 5 mm height and of 6 mm diameter. The powder was kept under dry argon atmosphere at all times.

A high-resolution focusing spectrometer is used to energy analyze the photons scattered by the sample at an angle of 135°. The Cauchois analyzing crystal is made of curved silicon, asymmetrically cut to employ the (620) reflection. Photons of the same energy are focused at a single point on the Rowland circle and detected by a position sensitive detector, filled with xenon at 4 atmospheres. The whole spectrum is collected at the same time. The entire-path of this scattered beam is maintained under vacuum.

The resolution function is deduced from the full width at half maximum (FWHM) of the thermal diffuse scattering (TDS) peak, which was 0.17 atomic units of momentum (a.u.). The separation between the experimental data points is equivalent to 0.03 atomic units when expressed in terms of the momentum scale. 10^6 counts were collected at the Compton peak. For the purpose of comparison, the Compton profile of C_{60} powder was also measured exactly under the same experimental conditions, with 10^6 counts at the Compton peak.

The experiments on K_3C_{60}, $CsRb_2C_{60}$, and Rb_4C_{60} were carried out using the Compton spectrometer of the high-energy beamline (Insertion Device 15B)[18] at the European Synchrotron Radiation Facility in Grenoble, France. The synchrotron radiation beam was monochromatized to select 55.8 (K_3C_{60} and Rb_4C_{60}) or 57.9 keV ($CsRb_2C_{60}$) photons and then focused on a powder sample. The powder was kept in a 1-mm diameter Lindemann capillary under Argon atmosphere. The collected Compton spectra were energy analyzed using the Ge 551 and Ge 440 Bragg reflections for incoming photons of energy respectively equal to 57.9 and 55.8 keV. Each spectrum achieved 10^6 counts at the Compton peak.

The energy-dependent resolution function is deduced from the full width at half maximum (FWHM) of the thermal diffuse scattering (TDS) peak, which was 0.25 atomic units of momentum (a.u.) for Rb_4C_{60} and $CsRb_2C_{60}$ and 0.2 a.u. for K_3C_{60}.

C. Data processing

After subtracting the background, the raw data were corrected for wavelength-dependent terms such as absorption (in the sample and analyzer), detector efficiency, and analyzer reflectivity predicted by kinematical theory.[19] The wavelength scale was then converted into a momentum scale. The spectra were normalized to the number of electrons per carbon atom. The contribution due to multiply scattered photons was subtracted from the measured profile, in order to obtain the total Compton profile. These multiple-scattering contributions were calculated using a Monte-Carlo simulation and taking into account beam polarization, sample geometry and density.[20]

In order to obtain the valence electrons Compton profile, the core electron profile was subtracted from the total measured profile. Under the impulse approximation, the core contribution is obtained from atomic wave functions. This approximation is valid only if the energy ΔE transferred from the photon to the ejected electron is large compared with the binding energy of the electron.[21]

In the 19.9-keV experiments, the Compton shift is 1200 eV, while the binding energies of potassium $2s$ and carbon $1s$ range between 200 and 300 eV. Therefore, it was necessary to move beyond the impulse approximation and to use the quasi-self-consistent-field method (QSCF) to obtain the core profiles for the C $1s$ and K $1s$ (Raman departure after 14 a.u.), $2s,2p,3s$ electrons.[22]

The potassium $3p$ core electrons will be treated as a ''pseudocore'' as described in the next section. After removing the core and pseudocore contributions, the remaining profile is normalized to the number of valence electrons per carbon atom, i.e., 4 in C_{60}, 4.05 in K_3C_{60}, and 4.067 in K_4C_{60}.

In the 55.8- and 57-keV experiments, impulse approximation Hartree-Fock Compton profiles for rubidium and cesium core electrons were subtracted from the total measured profiles.[23]

V. RESULTS AND DISCUSSION

Band-structure calculations, in general and those for C_{60} compounds in particular, are usually performed in order to obtain quantitative information about the charge distribution and Fermi surfaces (where applicable).[10–12] Our interest here is in the momentum space representation of the wave function, $\chi(p)$, leading to the electron momentum density and the related Compton profiles. While the calculated momentum density is obviously less intuitive than the real-space charge density, it has the advantage of (1) providing an integrated view of the characteristics of the electrons, (2) is sensitive to the contributions of the more delocalized electrons (valence and conduction), and (3) can be directly related to the results of Compton scattering experiments, thereby providing an excellent test for the calculated wave functions. The utility of this approach has already been demonstrated in intercalation compounds of graphite[24,25] and, more recently, for C_{60} (Ref. 5) and K_6C_{60}.[6]

A. Compton profile analysis

In the following, we will consider the experimental and theoretical Compton profiles of K_nC_{60} ($n=3,4$) minus that of C_{60} (normalized to 6 electrons). The difference profile is the result of three contribution:

(1) The K $3p$ electron contribution. The area of this contribution to the CP, is normalized to the number of K $3p$ electrons per carbon atom, i.e., 0.15, 0.2, and 0.3 in the low-energy side of CP ($q>0$), for $n=3$, 4, and 6, respectively.

(2) The conduction profile. This contribution is due to the electrons in the upper complex of three bands originating from the lowest unoccupied t_{1u} molecular orbitals in C_{60}. This complex forms the conduction band in K_nC_{60}, which becomes completely filled for $n=6$. It is normalized to 0.025, 0.0333 and 0.05 for $n=3$, 4 and 6, in the low energy side of CP ($q>0$).

(3) The distortion profile. This contribution is related to the distortion of the pristine C_{60} electronic density due to the presence of the K^+ ions. The net area under this profile is zero.

The comparison of experimental and theoretical K_nC_{60}-C_{60} ($n=3$ and 4) Compton profiles (with their own correct normalization) is shown in Fig. 1. The overall agreement between theory and experiment is good for K_3C_{60} and K_4C_{60}.

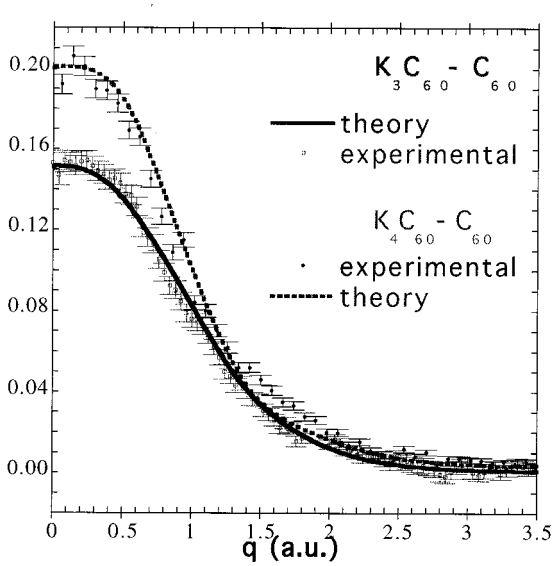

FIG. 1. Comparison between the experimental and theoretical valence-Compton profiles of K_nC_{60} minus C_{60} for $n=3$ and 4. The theoretical profiles (solid and dashed lines) are convoluted with the experimental resolution. The experimental results are represented by solid circles and open squares.

For K_3C_{60}-C_{60} and K_6C_{60}-C_{60} (Fig. 2 of Ref. 6), the experimental width is well reproduced by calculations. On the other hand, we notice that, in the K_4C_{60}-C_{60} case, the experimental Compton profile is narrower in the 0.5–1.5 a.u. region and larger for the 1.5 a.u.$<q<$3.5 a.u. region compared to the theory.

In order to be able to compare K_nC_{60} and C_{60} in a meaningful manner, it is necessary to subtract out the K3p contribution from both the calculated and measured profiles in K_nC_{60}. We define the Compton profile difference (CPD) as the sum of the conduction profile and the distortion profile, i.e., representing the effect of the additional electrons in the solid after the potassium intercalation, as well as the modifications in the pristine C_{60} electronic distribution brought about by intercalation. While we can separate these two contributions in our calculations, in the experiment it is obviously not possible.

B. The hybridization of carbon bands with K3p

We have shown that in the case of K_6C_{60},[6] it was possible to separate the contribution of K3p (pseudocore) from the calculated Compton profile in order to focus our attention on the bands resulting from C2s, C2p, and K4s. However, in the case of K_3C_{60} and K_4C_{60} this procedure is not possible due to the mixing of carbon bands with K3p orbitals. The same situation was encountered in all electron Korringa-Kohn-Rostoker band calculations in KC_8.[26] We stress that in pseudopotential calculations, K3p is included in the core and therefore their corresponding bands do not appear as a part of the valence complex.

In the following analysis, we will remove the contribution of K3p from the Compton profiles of K_3C_{60} and K_4C_{60} using the pseudocore obtained for K_6C_{60}.[6,27] Then we will obtain CPD's by taking the difference between the profiles of each of the two compounds and that of C_{60}.

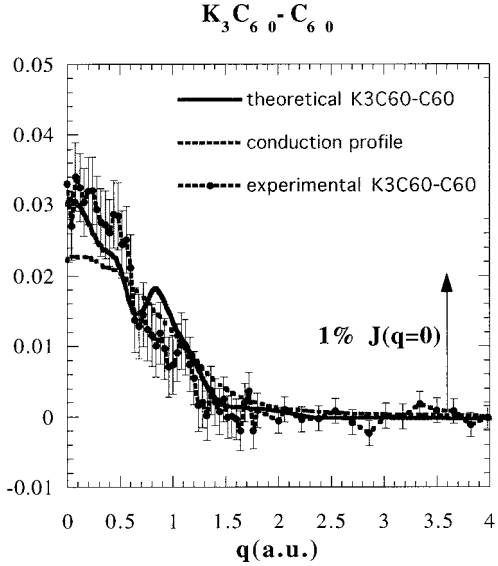

FIG. 2. Theoretical and experimental differences between valence-Compton profiles of K_3C_{60} and C_{60} (CPD). The potassium 3p contribution to the CP has been subtracted. The dashed line is the calculated conduction profile.

C. Comparison of Compton profile differences

In Figs. 2 and 3, we compare the experimental and theoretical CPD's ($n=3$ and 4) with the calculated conduction profile, which is positive for the two compounds and reaches zero near $q=3$ a.u.. We note that:

(1) in both cases, the experimental CPD is closer to the theoretical CPD than to the calculated conduction profile.

(2) the response of K_4C_{60} to the alkali intercalation presents a marked negative structure at 1 a.u., which is not observed in the K_3C_{60}-C_{60} CPD.

These facts lead to the conclusion that a nonzero distortion contribution to K_nC_{60}-C_{60} ($n=3$ and 4) CPD must be

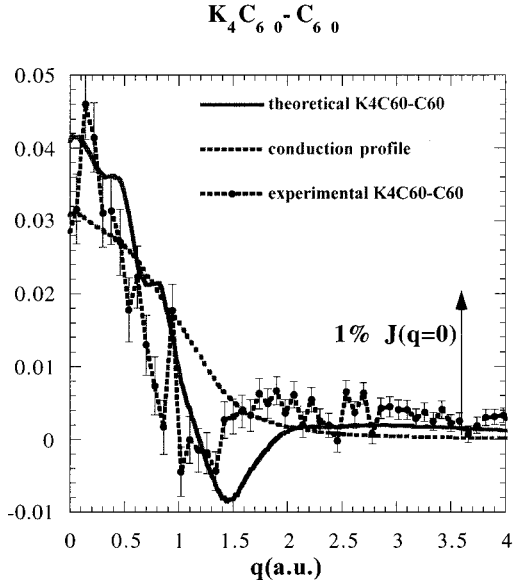

FIG. 3. Theoretical and experimental differences between valence-Compton profiles of K_4C_{60} and C_{60} (CPD). The potassium 3p contribution to the CP has been subtracted. The dashed line is the calculated conduction profile.

taken into account. These profiles can be compared to the K_6C_{60}-C_{60} CPD (Fig. 4 of Ref. 6) for which we concluded that the presence of K^+ ions leads to a small but clearly observable distortion of the charge density of C_{60} molecules in K_6C_{60}. The following points are worthy of special notice:

(1) For all the measured spectra the magnitude of this distortion contribution is well predicted by calculations even if it is small compared to the total Compton Profile.

(2) The calculations do not reproduce completely the experimental K_4C_{60}-C_{60} CPD: the latter is narrower for $0.5\,\text{a.u.} < q < 1.3\,\text{a.u.}$.

(3) compared to the K_4C_{60}-C_{60} CPD, the K_3C_{60} results present a better agreement between theory and experiment: the marked structure around 1 a.u. is absent in the K_3C_{60} case and the profile is always positive. This fact leads to the conclusion that, in this material, a smaller distortion contribution to CPD is present.

(4) Compton scattering can, in principle, detect the insulating character of K_4C_{60} and K_6C_{60} and the metallic character of A_3C_{60}. Chou, Cohen, and Louie[25] and Rabii, Chomilier and Loupias[25] have shown that for LiC_6 and LiC_{12} there is an oscillation in the *c*-axis profile because of the maxima and minima in the cross section of the Fermi surface and the resulting periodic variation of this cross section in the periodic zone scheme. The periods of these oscillations are 0.9 and 0.5 a.u. for LiC_6 and LiC_{12}, respectively. In K_6C_{60}, we should have no oscillation since there is no Fermi surface. The calculations give metallic behavior for K_3C_{60} and K_4C_{60} so there should be some oscillation of a period equal to the reciprocal vector in the direction of the scattering vector.

Since the reciprocal lattice vectors in K_nC_{60} are much shorter than in LiC_6 and LiC_{12}, the period of these oscillations will be smaller. Now, if K_4C_{60} is really an insulator, the measured difference profile (K_4C_{60}-C_{60}) should have no oscillations in the low q region while for K_3C_{60} we should observe oscillations.

Unfortunately these oscillations cannot be measured in our experiments for two reasons

(a) The period is smaller than the experimental resolution (0.17–0.20 a.u.).

(b) The Compton profile of powder samples is the average of many directional profiles: this fact leads to more than one set of oscillations.

In order to measure the metallic-insulator state of intercalated fullerenes, very high resolution measurements on single crystals should be performed.

D. Distortion contribution

In order to analyze the distortion contribution to the measured Compton profiles, in Fig. 4, we compare the calculated distortion profiles for the three compounds (the difference profiles are not convoluted by the experimental resolution). We note that the overall behavior of the distortion in K_4C_{60} is similar to K_6C_{60}. The distortion profile is positive at low q (denoting electron delocalization), shows a structure around $q = 0.8$ a.u and approaches zero for q larger than 3 a.u. Such general behavior is typical of a delocalization of π orbitals in real space. It is well known that π orbitals that are parallel to the scattering vector lead to a Compton profile that is zero at $q = 0$ and have a non zero momentum maximum in the region of $q = 1$ a.u. On the other hand, π orbitals that are perpendicular to the scattering vector, lead to a Compton profile whose maximum is at $q = 0$, and have no structure in the region of $q = 1$ a.u.. Since C_{60} molecules are almost spherical, some of the π orbitals will be parallel, some perpendicular, and some at intermediate angles with respect to the scattering vector. The delocalization of these orbitals in real space leads to the shift of their contribution to CP towards lower q values (momentum space). So, the $q = 0$ maximum reflects the shift, to lower q, of the contribution of π orbitals which are perpendicular to the scattering vector and the $q = 0.8$ structure reflects the shift, to lower q, of 1 a.u. maximum CP, derived from the π orbitals parallel to the scattering vector.

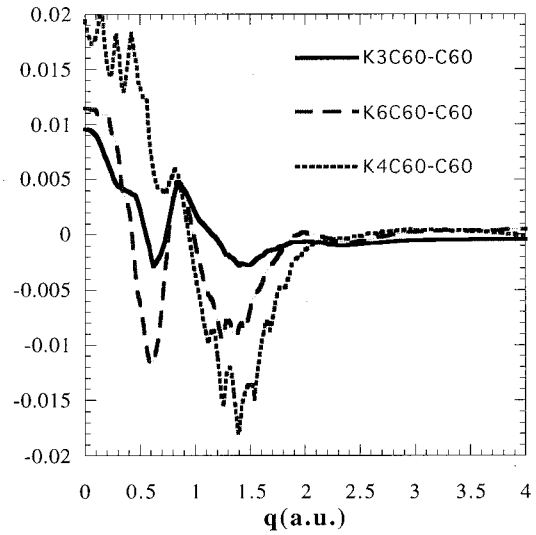

FIG. 4. Calculated distortion profiles for K_nC_{60} for $n = 3$, 4, and 6. These profiles are not convoluted with the experimental resolution function.

In order to explain the less marked behavior of the distortion contribution to CPD, in K_3C_{60} case, we remark that the potassium environment around a C_{60} molecule in K_4C_{60}, can be viewed as that in K_6C_{60}, but with some vacancies. On the other hand, in K_3C_{60} it presents a very different structure: potassium ions fill the tetrahedral and octahedral sites of a fcc structure. As a consequence, the free volume for the potassium ion is larger in K_3C_{60} than in the other compounds: 178 $Å^3$ compared to 143 $Å^3$ (K_4C_{60}) and 91.6 $Å^3$ (K_6C_{60}). We can assume that in these intercalated molecular materials, this parameter reflects the molecular charge density distortion.

Furthermore, we have noted that the calculated distortion (compared to pristine C_{60}) is more important in K_4C_{60} than in K_6C_{60}: the tetragonal symmetry of the former material, in contrast to the cubic structure of K_6C_{60} and pristine C_{60}, can be invoked as an explanation.

E. Comparison with rubidium and cesium intercalated compounds

In order to make a meaningful comparison of the results for $CsRb_2C_{60}$ and Rb_4C_{60} with those of K_nC_{60} ($n = 3$ and 4), we obtain CPD for these compounds by subtracting the Compton profile of C_{60} and of the core electrons[23] of Rb and

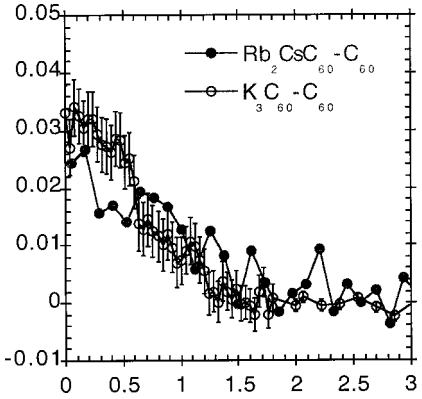

FIG. 5. The measured difference between valence-Compton profiles of Rb_2CsC_{60} and C_{60} (CPD) compared to K_3C_{60}-C_{60}. The alkali core contribution to the CP has been subtracted.

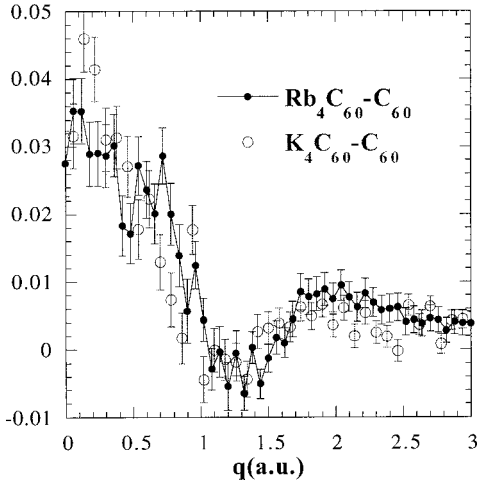

FIG. 6. The measured difference between valence-Compton profiles of Rb_4C_{60} and C_{60} (CPD) compared to K_4C_{60}-C_{60}. The alkali core contribution to the CP has been subtracted.

Cs from the total $CsRb_2C_{60}$ and Rb_4C_{60} profiles. These results are presented in Figs. 5 and 6 where they are compared to the CPD's of potassium intercalated compounds. We can conclude that the CPD's of A_nC_{60} ($n=3$ and 4) compounds do not depend on the nature of the intercalated ions but rather on their number. The trends in the experimental heavy ions intercalated CPD's reproduce the figures discussed previously: i.e., A_4C_{60}-C_{60} CPD's show a marked structure at 1 a.u., which is absent in the A_3C_{60} case. We note that the width of the measured Rb_4C_{60}-C_{60} CPD is larger than that of K_4C_{60}-C_{60}, but still narrower than the theoretical K_4C_{60}-C_{60} CPD.

VI. CONCLUSIONS

We have measured the Compton profiles of K_nC_{60} ($n=3,4,6$[6]), $CsRb_2C_{60}$ and Rb_4C_{60} and obtained CPD between these compounds and pristine C_{60}. In the case of potassium intercalated compounds, the simulation of CPD's by *ab initio* calculations can describe the main trends of the experimental results; this permits us to isolate the contribution of the distortion of the C_{60} orbitals for each compound and to compare them, as a function of potassium intercalation: K_3C_{60} presents a distortion that is less important than in the K_4C_{60} and K_6C_{60} compounds and this is probably linked to the lower concentration of intercalated ions. For K_4C_{60}, as in the case of K_6C_{60}, the main structures of the calculated distortion profiles are explained by an overall delocalization of charge away from the C-C bonds. However, in the case of K_4C_{60}, the comparison between the widths of the calculated and measured CPD's is not satisfactory: the calculated width is larger than the experimental one. For K_3C_{60} and K_6C_{60} (Ref. 6) we have obtained a better agreement between theory and experiment.

Furthermore, similar measurements performed on heavy-ion intercalation compounds (Rb_4C_{60} and $Rb_2C_8C_{60}$) show clearly that the CPD depends on the number of ions and not on their nature.

We put forward two possible hypotheses in order to explain the mismatch between theoretical and experimental CPD's of K_4C_{60}.

(1) The orientations of C_{60} molecules in these compounds vary with n. Only in the case of K_6C_{60}, where the molecules are orientationally ordered, the calculation was performed for the actual orientation. In A_3C_{60} and A_4C_{60} compounds, the present calculations are not able to take into account the randomly occupied sites with two inequivalent orientations.

(2) Jahn-Teller effect for the negatively charged C_{60} molecule in the solid. In its ground state, the neutral C_{60} molecule possesses a closed shell electronic structure. The lowest unoccupied molecular orbital is threefold degenerate and a Jahn-Teller interaction will be possible when C_{60} is excited to this orbital and for anions such C_{60}^{-}, C_{60}^{3-} and C_{60}^{4-}. O. Gunnarsson *et al.*[28] have compared experimental and theoretical photoemission spectra for C_{60}^{-} and deduced that the inclusion of the Jahn-Teller effect in the calculations is essential.

In order to take into account such a phenomenon in solid intercalated A_nC_{60} ($n=3$ and 4)—where the molecule is charged by alkali ions—local density approximation calculations should be performed allowing atoms to relax from their equilibrium position. Our calculations are performed for a rigid configuration of the atoms in the molecule and this effect, if present, is neglected. We note that in the K_6C_{60} case, the complex of three bands originating from the lowest unoccupied t_{lu} molecular orbitals of C_{60} is filled and no Jahn-Teller effect is expected.

ACKNOWLEDGMENTS

We would like to thank Dr. A. Issolah, for providing OSCF calculations of the contribution of core electrons to the Compton profile, P. Suortti and J. Moscovici for useful discussions. We are grateful to C. Hérold, J. F. Marêché, Ph. Lagrange (LCSM, Univ. Nancy I, BP 239, 54506 Vandoeuvre-Cedex, France) and to L. Forro (Physics Dept./ IGA Ecole Polytechnique Federale de Lausanne Switzerland) for providing samples. Two of the authors (G. L. and S. R.) would like to acknowledge the support of NATO, under Grant No. CRG 920139.

*Also at Laboratoire pour l'Utilisation du Rayonnement Electromagnetique, bât. 209, Univ. Paris-Sud, 91405 Orsay cedex, France.

[1] O. Zhou, J. E. Fischer, N. Coustel, S. Kycia, Q. Zhu, A. R. McGhie, W. J. Romanow, J. P. McCauley, A. B. Smith, and D. E. Cox, Nature (London) **351**, 462 (1991).

[2] P. W. Stephens, L. Mihaly, P. L. Lee, R. L. Whetten, S. M. Huang, R. Kaner, F. Diederich, and K. Holczer, Nature (London) **351**, 632 (1991).

[3] C. H. Kuntscher, G. M. Bendele, and P. W. Stephens, Phys. Rev. B **55**, R3366 (1997).

[4] O. Chauvet, G. Oszlàny, L. Forro, P. W. Stephens, M. Tegze, G. Faigel, and A. Jànossy, Phys. Rev. Lett. **72**, 2721 (1994).

[5] J. Moscovici, G. Loupias, S. Rabii, S. Erwin, A. Rassat, and C. Fabre, Europhys. Lett. **31**(2), 87 (1995).

[6] M. Marangolo, J. Moscovici, G. Loupias, S. Rabii, S. Erwin, C. Hérold, J. F. Marêche, and Ph. Lagrange, Phys. Rev. B **58**, 7593 (1998).

[7] P. Eisenberger and P. M. Platzman, Phys. Rev. A **2**, 415 (1970).

[8] M. J. Cooper, Rep. Prog. Phys. **48**, 415 (1985).

[9] L. Mendelsohn and V. H. Smith, *Compton Scattering*, edited by Brian Williams (Mc Graw-Hill, New York, 1977).

[10] S. C. Erwin, in *Buckminsterfullerenes*, edited by W. E. Billups and M. A. Ciufolini (VCH, New York, 1993), p. 217.

[11] S. C. Erwin and W. E. Pickett, Science **254**, (1991).

[12] S. C. Erwin and C. Bruder, Physica B **199&200**, 600 (1994).

[13] S. C. Erwin, M. R. Pederson, and W. E. Pickett, Phys. Rev. B **41**, 10 437 (1992).

[14] G. Lehmann and M. Taut, Phys. Status Solidi B **87**, 221 (1978).

[15] P. Lagrange, D. Bégin, C. Hérold, J. F. Marêché, Images de la Recherche, Départements Sciences Physiques et Mathématiques et Sciences Chimiques du CNRS ''Les Fullerènes'' 66 (1997); J. Moscovici, thèse de l'Université Paris VI, 1994.

[16] G. Loupias, J. Petiau, A. Issolah, and M. Schneider, Phys. Status Solidi B **102**, 79 (1980).

[17] J. Frouin, Y. Garreau, G. Loupias, D. Raoux, and J. Tarbès, Nucl. Instrum. Methods Phys. Res. A **266**, 484 (1988).

[18] P. Suortti, Th. Buslaps, P. Fajardo, V. Honkimäki, M. Kretzschmer, U. Lienert, J. E. McCarthy, M. Renier, Th. Tschentscher, and T. Meinander, J. Synchrotron Radiat. **6**, 69 (1999).

[19] F. Balibar, Y. Epelboin, and C. Malgrange, Acta Crystallogr., Sect. A: Cryst. Phys., Diffr., Theor. Gen. Crystallogr. **31**, 836 (1975); E. Erola, V. Eteläniemi, P. Suortti, P. Pattison, and W. Thomlinson, J. Appl. Crystallogr. **23**, 35 (1990).

[20] J. Chomilier, G. Loupias, and J. Felsteiner, Nucl. Instrum. Methods Phys. Res. A **235**, 603 (1985).

[21] W. M. DuMond, Phys. Rev. **33**, 643 (1929); **36**, 146 (1930).

[22] A. Issolah, B. Lévy, A. Beswick, and G. Loupias, Phys. Rev. A **38**, 4509 (1988); A. Issolah, Y. Garreau, B. Lévy, and G. Loupias, Phys. Rev. B **44**, 11 029 (1991).

[23] F. Biggs, L. B. Mendelsohn, and J. B. Mann, At. Data Nucl. Data Tables **16**, 201 (1975).

[24] G. Loupias, J. Chomilier, and D. Guérard, J. Phys. Lett. (Paris) **45**, L301 (1984); M. Y. Chou, S. Louie, M. L. Cohen, and N. Holzwarth, Phys. Rev. B **30**, 1062 (1984); G. Loupias, J. Chomilier, and D. Guérard, Solid State Commun. **55**, 299 (1985).

[25] M. Y. Chou, M. L. Cohen, and S. G. Louie, Phys. Rev. B **33**, 6619 (1986); S. Rabii, J. Chomilier, and G. Loupias, *ibid.* **40**, 10 105 (1989).

[26] D. P. DiVincenzo and S. Rabii, Phys. Rev. B **25**, 4110 (1982).

[27] As for K_6C_{60}, for polymerized K_1C_{60} (to be published) it has been possible to separate the K3p contribution to CP. The difference between the two contributions is very small: ± 0.001, in the same scale of figures plotted in this article, for $0<q<2$, for 6 K3p electrons. This result suggests that our K3p contribution evaluation is correct also for the other measured materials.

[28] O. Gunnarsson, H. Handschuh, P. S. Bechthold, B. Kessler, G. Gantför, and W. Eberhardt, Phys. Rev. Lett. **75**, 1875 (1995).